International Journal of Pharmaceutical Science and Research
ISSN: 2455-4685; Impact Factor: RJIF 5.28
Received: 08-01-2019; Accepted: 10-02-2019
www.pharmacyjournal.net
Volume 4; Issue 2; April 2019; Page No. 07-12

Synchronous fluorescence and molecular docking to explore the mechanism of meloxicam and lipase

Xu Cheng[1], Baosheng Liu[2], Hongcai Zhang[3]
[1-3] College of Chemistry & Environmental Science[1], Hebei University, Baoding, Hebei, China

Abstract
The interaction between lipase and rheumatoid arthritis drug meloxicam (MEL)were studied by synchronous fluorescence method under pH=7.40. The results showed that MEL quenched the fluorescence of Tyr residues and Trp residues in a static quenching manner. Fluorescence quenching ratio showed that the binding position was closer to the Trp residue. The binding rate of MEL to Tyr residue in lipase was *W*(*Q*)=1.10%~0.77%, *W*(*B*)=1.10%~30.96%, and the binding rate to Trp residue *W*(*Q*)= 1.64%~1.01%, *W*(*B*)= 1.64%~40.23%, respectively, the binding model was established. The main types of MEL and lipase binding system are hydrophobic interaction and hydrogen bonding, and there is no synergistic effect in the binding. The molecular docking results indicate that the optimal binding position is near the active center of lipase, and the combination of the two changes. In the microenvironment at the active center, the combined reaction may have an effect on the digestion of fatty substances.

Keywords: synchronous fluorescence method, meloxicam, lipase, amino acid residue

1. Introduction

The text must be in English. NSAIDs (non-steroidal anti-inflammatory drugs) are compounds which are widely used in the symptomatic treatment of inflammatory diseases, such as rheumatoid arthritis and they act by reducing the pain and edema. The mechanism of action of these drugs is the inhibition of the enzyme cyclooxygenase (COX), causing a decrease in the biosynthesis of the prostaglandins (PGs), which are important chemical mediators of inflammation. However, the chronic use of NSAIDs may cause many collateral effects such as gastritis, ulcers, and kidney and liver problems [1]. There are several classes of NSAIDs, and they exhibit different chemical structures. One such class is oxicams (e.g., piroxicam, tenoxicam and meloxicam), which are drugs that were developed in the 1980s by Pfizer™ [2].

MEL is 4-hydroxy-2-methyl-N-(5-methyl-2-thiazolyl)-2H-1,2-benzothiazine-3-carboxamide-1,1-dioxide [3], and its structure is shown in Fig. 1. Amid NSAIDs is MEL, which is a superior selective cyclooxygenase (COX)-2 inhibitor through less gastrointestinal toxicity than nonselective NSAIDs [4]. However, using MEL long-term will still seriously affect the digestive function of the gastrointestinal tract.

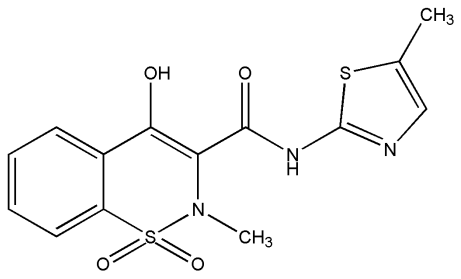

Fig 1: Chemical structure of MEL

Lipase is a hydrolase that decomposes triacylglycerol. It is an intracellular enzyme. Its catalytic site contains a nucleophilic catalytic triad (SHD or SHE). The catalytic site is buried inside the molecule and the surface is formed by relatively hydrophobic amino acid residues. Covered by a spiral lid structure to protect the catalytic part of the triplet [5]. Human lipase is mainly secreted by pancreatic acinar cells, so it is also called pancreatic lipase, and plays a role in digesting fat in the duodenum. It plays an important role in the absorption of triglycerides in the small intestine. Hydrolyzed triglyceride is converted into Glycerin and fatty acids are absorbed by the body [6] and play an important role in the process of digestion and absorption. Zhao Lining *et al*. [7] studied the interaction of three mercaptopropionic acid-terminated CdTe quantum dots with lipase, and proved that three mercaptopropionic acid-terminated CdTe quantum dots can cause toxic side effects on lipase; Zhang Rui *et al*. [8] studied the interaction of bisphenol A with lipase in vitro to better understand the toxicity and toxicity mechanism of bisphenol A.

At present, the methods for exploring the mechanism of drug and protein reaction are mainly to investigate the excitation wavelengths of 280 nm and 295 nm, and the fluorescence of the protein is quenched with the drug concentration, which is the overall effect of the study of drugs and proteins [9]. Synchro fluorescence combines the advantages of good selectivity, high sensitivity, narrowing the band and reducing scattering interference [10]. In the study of the mechanism of drug and protein reaction, the synchronous fluorescence method is mainly used to synchronize the displacement of fluorescent peaks and investigate changes in protein conformation [11]. At present, the use of simultaneous fluorescence and molecular docking techniques to study the interaction mechanism between meloxicam and Tyr residues and Trp residues in lipase molecules has not been reported. The binding rate of the system obtained based on the experimental results is helpful to study the combination of drug molecules and proteins, as well as the pharmacological and pharmacological effects of drugs, while the fluorescence quenching ratio fraction and

molecular docking model can reveal drug molecules and amino acids at a deeper level. The reaction mechanism of residues provides a reference for the study of the combination of small molecule drugs and proteins.

2. Materials and Methods

2.1 Apparatus

These fluorescence spectra were acquired with a Shimadzu RF-5301PC spectrofluorophotometer. All pH measurements were made with a pHS-3C precision acidity meter (Leici, Shanghai, China). All temperatures were controlled by a SYC-15$_B$ superheated water bath (Sangli, Nanjing, China).

2.2 Materials

Porcine pancreatic lipase (PPL) was purchased from Sigma-Aldrich (purity grade inferior 99%, Shanghai, China), preparation of PPL standard solution 5.0×10^{-6} mol/L. Preparation of MEL (CAS#, 71125-28-7) standard solut ion 4.0×10^{-4} mol/L. Tris-HCl buffer solution was used to keep the pH of the solution at 7.40, and NaCl (0.10 mol/L) solution was used to maintain the ionic strength of the solution. All other reagents were of analytical grade, and all aqueous solutions were prepared with fresh double-distilled water and stored at 277 K. The fluorescence intensity measured in the experiment was corrected by the "internal filter effect" Eq. (1) [12]:

$$Fcor = Fobs \times e^{(A_{ex}+A_{em})/2} \quad (1)$$

Where F_{cor} and F_{obs} are the corrected and observed fluorescence intensities, respectively, and A_{ex} and A_{em} are the absorbance values of MEL-PPL system at excitation and emission wavelengths, respectively. The fluorescence intensity used in this article was corrected.

2.3 Synchronous fluorescence experiment

1.0 mL Tris-HCl buffer solution (pH=7.40), 2.0 mL PPL (5.0×10^{-6} mol/L), and different volume of MEL were added into 10 mL colorimetric tube successively. The samples were diluted to scaled volume with double-distilled water, mixed thoroughly by shaking, and kept static for 30 min at different temperatures (298 K, 310 K and 318 K). Place the prepared solution in a 1.0 cm quartz cuvette and set the slit width to 5 nm. At the same time fixed $\Delta\lambda$ =15 nm or $\Delta\lambda$=60 nm, the synchronous fluorescence spectra of MEL and PPL were recorded.

2.4 Molecular docking

The crystal structure of PPL (PDB ID: 1GPL) was obtained in a Protein Data Bank, and the structure of the MEL was processed using the software ChemDraw Pro 14.0 and the software ChemBio 3D Ultra 14.0. Molecular docking of MEL and PPL in AutoDock 4.2.6 software uses genetic algorithms to calculate possible conformations with proteins and drug molecules [13].

3. Results & Discussion

3.1 Synchronous fluorescence experiment

For synchronous fluorescence spectra of proteins, when the $\Delta\lambda$ value between the excitation and emission wavelengths is stabilized at 15 or 60 nm, the synchronous fluorescence gives characteristic information for Tyr or Trp residues [14]. As shown in Fig. 2, the addition of MEL quenched the fluorescence of the Tyr residue or the Trp residue, and the degree of quenching was further enhanced as the drug concentration increased. The results indicated that MEL interacted with PPL to form a stable conjugate. A blue shift of the λ_{max} of Tyr residues and Trp residues were observed. The blue shift of Tyr residues and Trp residues implied that the microenvironment of these residues become more hydrophobic and polarity enhancement. The results indicated that the addition of MEL caused a change in the conformation of the PPL.

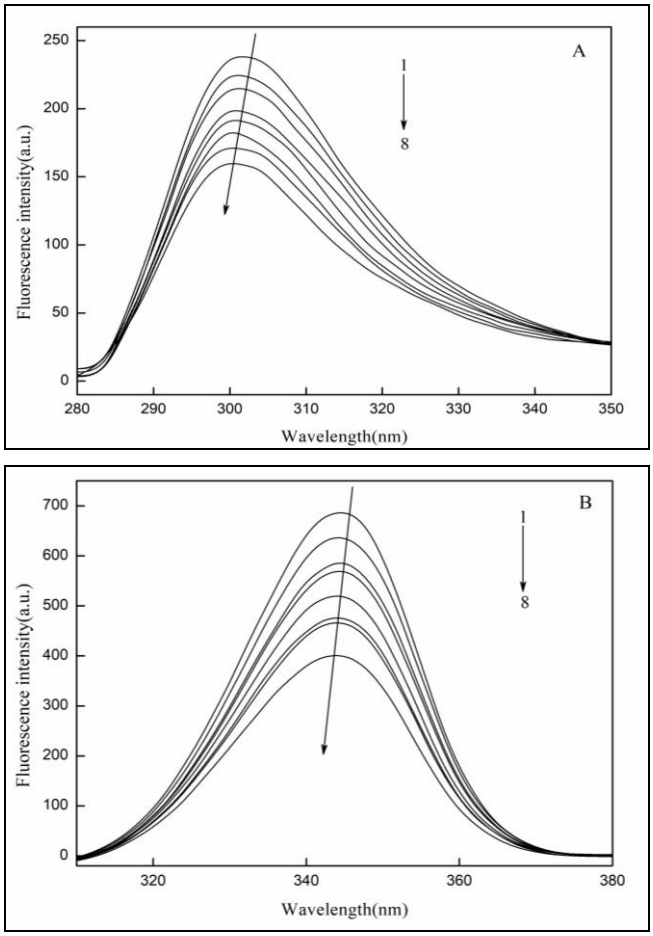

Fig 2: Synchronous fluorescence spectra of MEL-PPL system (T=310 K). (A) Δλ=15 nm, (B) Δλ=60 nm. C_{PPL}=1.0×10-6 mol/L, 1~8 C_{MEL}= (0, 0.1, 0.2, 0.5, 1.0, 2.0, 3.0, 4.0) $\times10^{-5}$ mol/L

Table 1: Quenching reactive parameters of MEL-PPL system at different temperatures

Δλ (nm)	T/(K)	K_q (L/mol·s)	K_{sv} (L/mol)	r_1	K_a (L/mol)	n	r_2
15	298	1.34×10^{12}	1.34×10^{4}	0.9969	1.41×10^{4}	0.98	0.9915
	310	1.12×10^{12}	1.12×10^{4}	0.9957	1.13×10^{4}	1.12	0.9963
	318	0.91×10^{12}	0.91×10^{4}	0.9946	0.88×10^{4}	0.91	0.9938
60	298	1.79×10^{12}	1.79×10^{4}	0.9955	1.95×10^{4}	0.95	0.9941
	310	1.53×10^{12}	1.53×10^{4}	0.9913	1.68×10^{4}	1.10	0.9947
	318	1.28×10^{12}	1.28×10^{4}	0.9937	1.27×10^{4}	0.93	0.9919

r_1 is the linear relative coefficient of F_0/F~$[L]$; r_2 is the linear relative coefficient of $\lg[(F_0\text{-}F)/]$~$\lg\{[L]\text{-}n[B_t](F_0\text{-}F)/F_0\}$

To confirm the quenching mechanism, the fluorescence quenching data were analyzed using the Stern-Volmer Eq. (2) [15]:

$$F_0/F = 1 + K_q\tau_0[L] = 1 + K_{SV}[L] \quad (2)$$

Where F_0 and F represent the fluorescence signals in the

absence and presence of quencher, respectively. τ_0 is the average lifetime of fluorescence without quencher, which is about 10^{-8} s. K_{sv} is the Stern-Volmer quenching constant. K_q is the bimolecular quenching constant, and [L] is the concentration of MEL. The results were shown in Table 1. Table 1 showed that the values of K_q decreased with increasing temperature in all systems. In addition, all the values of K_q were much greater than the maximum scatter collision quenching constant values of various quenchers (2×10^{10} L/mol·s) in different temperatures. The relationship between the K_{sv} value of the system and the temperature was negatively correlated, so it could be inferred that the annihilation mode of the MEL-PPL system was static quenching [16]. The relationship between fluorescence intensity and the concentration of quencher can usually be described using Eq. (3) to obtain the binding constant (K_a) and the number of binging sites (n):

$$lg\left(\frac{F_0-F}{F}\right) = n\,lg\,K_a + n\,lg\left\{[L] - n\frac{F_0-F}{F_0}[B_t]\right\} \qquad (3)$$

Where [B_t] is the concentration of PPL. On the assumption that n in the bracket is equal to 1, the curve of lg(F_0-F)/F versus lg{[L]-n[B_t](F_0-F)/F} is drawn and linearly fitted, then the value of n can be obtained from the slope of the plot. On the basis of value of n obtained, the binding constant K_a can also be determined. The results were listed in the Table 1. The results showed that all the values of n were approximately equal to 1 at different temperatures, implying that there was just one high affinity binding site existing in PPL [17]. Meanwhile, the binding constant between MEL and PPL decreased with an increasing temperature, further suggesting that the quenching of MEL-PPL system was a static process. It could be further seen from the data in the table that the K_a value at $\Delta\lambda$ = 15 nm is significantly smaller than the K_a value at $\Delta\lambda$ = 60 nm, which indicated that the MEL reacts more strongly with the Trp residue.

The degree of decrease in the synchrotron fluorescence intensity is represented by the quenching ratio R_{SFQ}, R_{SFQ}=1−F/F_0 [18]. Calculate the $R_{SFQ(Tyr)}$ and $R_{SFQ(Trp)}$ values under the same temperature and drug concentration, and define $N_{SFQR(Tyr)}$=($R_{SFQ(Tyr)}$/($R_{SFQ(Tyr)}$ + $R_{SFQ(Trp)}$)% is the of the fluorescence quenching ratio fraction of the Tyr residue and $N_{SFQR(Trp)}$=100%-$N_{SFQR(Tyr)}$ is the fluorescence quenching ratio fraction of the Trp residue.

The $N_{SFQR(Tyr)}$ at C_{MEL}/C_{PPL}= (2, 5, 10, 20, 30, 40) at 310 K were: 44.08%, 45.12%, 45.66%, 46.47%, 46.90%, 47.45%, and the average result was 45.95%. $N_{SFQR(Trp)}$ were: 55.92%, 54.88%, 54.34%, 53.53%, 53.10%, 52.55%, and the average result was 54.05%. The results indicated that both Tyr residues and Trp residues were involved in the reaction, and $N_{SFQR(Trp)}$> $N_{SFQR(Tyr)}$, indicating that the reaction position should be closer to Trp, further indicating that MEL reacts more strongly with Trp residues.

3.2 MEL-PPL system binding rate

According to the experimentally obtained K_a, the drug binding rate and protein binding rate of MEL and PPL can be calculated [19].

The binding rate of drug can be given `by Eq. (4):

$$W(Q) = \frac{x}{Q}\times 100\% = \frac{K_a(Q+B)+1-\sqrt{Ka^2(Q-B)^2+2K_a(Q+B)+1}}{2K_aQ}\times 100\% \qquad (4)$$

The binding rate of protein can be given by Eq. (5):

$$W(B) = \frac{x}{B}\times 100\% = \frac{K_a(Q+B)+1-\sqrt{Ka^2(Q-B)^2+2K_a(Q+B)+1}}{2K_aB}\times 100\% \qquad (5)$$

Q represents the total concentration of MEL; B represents the total concentration of PPL. At 298K, 310K and 318K, the drug binding rate W(Q) of Tyr residues in MEL and PPL was calculated according to formulas (4) and (5), respectively, from 1.34% to 0.88% (298K), 1.10%~0.77%(310K), 0.87%~0.65%(318K), protein binding rate W(B) was 1.34%~35.36%(298K), 1.10%~30.96%(310K), 0.87%~25.91%(318K). The drug binding rate W(Q) of Trp residues in MEL and PPL was 2.01%~1.12% (298K), 1.64%~1.01% (310K), 1.29%~0.86% (318K), protein binding rate W(B) were respectively 2.01%~45.13% (298K), 1.64%~40.23% (310K), 1.29%~34.53% (318K). At three temperatures, the drug binding rate and protein binding rate of Tyr residues and Trp residues in MEL and PPL decreased with increasing temperature, and the free drug and protein content increased with temperature. The results indicated that the stability of the combined system decreases as the temperature increased. The binding rate of MEL to Trp residues at different temperatures was higher than that of MEL to Tyr residues, indicating that MEL reacted more strongly with Trp residues. This view was consistent with the results of simultaneous fluorescence experiments.

Assumed the ratio of total concentration of drug to total concentration of protein was R, R = Q/B. According to the relationship between W(Q), W(B) and R, the results were shown in Fig. 3. It could be seen from Figure 3 that with the increase of MEL concentration, W(Q) showed a weak downward trend, and W(B) showed a significant increase trend. Taking 310K data close to human body temperature as an example: The W(Q) of MEL and Tyr residues and Trp residues were 1.10%~0.77% and 1.64%~1.01%, respectively, which indicated that MEL increased with the addition of MEL. Interaction with PPL has little effect on the efficacy of MEL. The W(B) of MEL and Tyr residues and Trp residues were 1.10%~30.96% and 1.64%~40.23%, respectively. This result indicated that the protein binding rate changed greatly with the increased of MEL addition, possibly to pancreatic lipase. The activity had an effect, which affected the digestion and absorption of fat. Therefore, in order to reduce the impact of MEL on digestive function, it is necessary to properly control the drug intake during the administration of MEL.

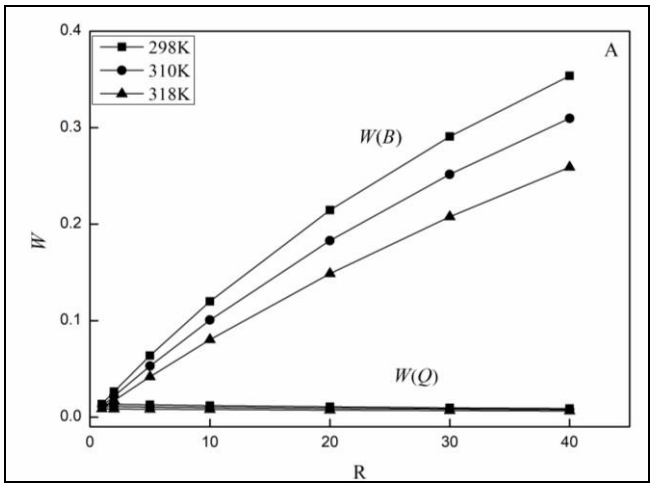

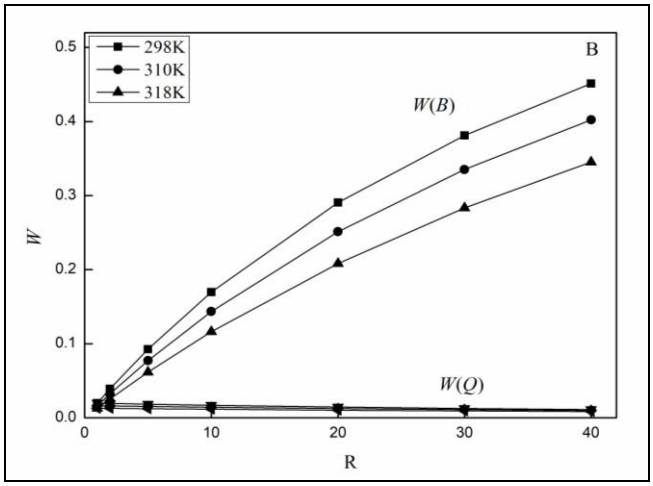

Fig 3: Binding rate of MEL to Tyr residue and Trp residue of PPL at different temperatures. (A) $\Delta\lambda$=15 nm, (B) $\Delta\lambda$=60 nm

3.3 Type of interaction force of MEL-PPL system and Hill's coefficient

The signs and magnitudes of the thermodynamic parameters (ΔH, ΔS and ΔG) in the binding process of biomacromolecule with small molecule can be used to confirm the binding modes. These thermodynamic parameters can be calculated by the van't Hoff equations [20]:

$$R \ln K = \Delta S - \Delta H/T \quad (6)$$

$$\Delta G = -RT \ln K = \Delta H - T\Delta S \quad (7)$$

Where ΔH and ΔS represent the standard variation of the enthalpy and, respectively, entropy of the binding process. R is the gas constant (R=8.314 J·mol^{-1}·K^{-1}), T is the absolute temperature. Based on the linear fit plot of $R\ln K$ versus 1/T, the ΔH and ΔS values can be obtained. The results were shown in Table 2. Obviously, the binding interaction of MEL with PPL was spontaneous due to the negative value of ΔG under the studied temperature ranges. The positive value of ΔS is often attributed to hydrophobic interaction. However, the negative value of ΔH cannot be regarded as evidence for electrostatic interactions because in the case of electrostatic interactions ΔH is very much small and close to 0, while the negative value of ΔH can be mainly attributed to hydrogen-binding interactions [21-23]. Therefore, the primary binding forces for the binding interaction of MEL with PPL were hydrophobic interactions and hydrogen bonding interactions. From the data in the Table 2, it can be found that the value of ΔG at $\Delta\lambda$=60 nm is smaller than the value of ΔG at $\Delta\lambda$=15 nm, further indicating that the reaction between MEL and Trp residues is stronger.

Table 2: The thermodynamic parameters of MEL-PPL at different temperatures

System	T/(K)	K_a/(L/mol)	ΔH/(kJ/mol)	ΔS/(J/mol·K)	ΔG/(kJ/mol)
$\Delta\lambda$=	298	1.38×10^4	-17.26	21.32	-24.49
15 nm	310	1.13×10^4		21.91	-25.08
	318	0.88×10^4		21.22	-24.98
$\Delta\lambda$=	298	1.97×10^4		26.4	-24.49
60 nm					
	310	1.68×10^4	-16.63	27.23	-25.08
	318	1.27×10^4		26.26	-24.98

It is generally acknowledged that the electrostatic interaction plays the auxiliary role in the binding process of bound ligands to protein. But, if the electrostatic binding interaction is predominant role in the binding process, the strength of total interaction will decrease upon the addition of NaCl to the system. To confirm whether there is electrostatic interaction between MEL and PPL, the effect of ionic strength on the binding force was explored [24].

The results were shown in Fig.4. With the increased of NaCl concentration, the ratio of F/F_0 was basically unchanged. The degree of binding between MEL and PPL system did not change significantly with the increased of ionic strength, which indicated that there was no obvious electrostatic interaction between MEL and PPL system. This conclusion was the same as the conclusion of the thermodynamic constant.

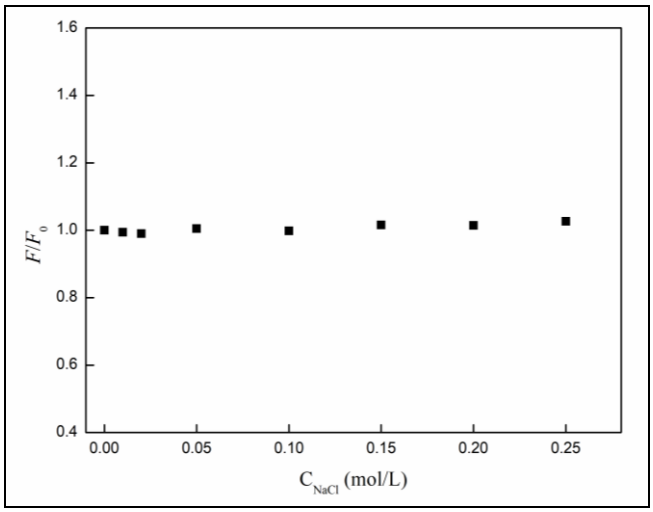

Fig 4: Fluorescence intensity of MEL-PPL system as a function of NaCl concentration (T=310K). C_{PPL}=1.0×10^{-6} mol/L, C_{MEL}=1.0×10^{-5} mol/L, C_{NaCl}=(0, 0.1, 0.2, 0.5, 1.0, 1.5, 2.0, 2.5, 3.0) ×10^{-1}mol/L

The synergy of drugs can be obtained by the following equation [25]:

$$lg\{Y/(1-Y)\} = lg\, K\, a + nH\, lg[L] \quad (8)$$

Where K_a is the binding constant, Y is the fractional binding saturation, n_H is the Hill's coefficient and [L] is the concentration of MEL. Hill's coefficient is greater than 1, which exhibits positive cooperativity and its role is enhanced with increasing n_H. Conversely, Hill's coefficient is less than 1, which exhibits negative cooperativity and its role is enhanced by decreasing n_H. A coefficient of 1 indicates non-cooperative reaction [26].

For fluorescence measurement:

$$Y/(1-Y) = Q/(Qm - Q) \quad (9)$$

$$Q = 1 - F/F_0 \quad (10)$$

Where $1/Q_m$ is intercept of the plot $1/Q$ versus $1/[L]$. According to the Eq. (8), Eq. (9) and (10), Hill's coefficient of MEL-PPL system can be gained from the slope of the plot of log [Y/(1−Y)] versus log[L]. The results were presented in Table 3. At different temperatures, the n_H value was approximately equal to 1, and the results indicated that

there was no synergy between MEL and PPL, indicating that the binding of PPL to subsequent ligands was not affected with the addition of MEL.

Table 3: Hill coefficient of MEL-PPL systems at different temperatures

T/K	Δλ = 15 nm		Δλ = 60 nm	
	n_H	r_3	n_H	r_3
298	1.05	0.9932	1.01	0.9931
310	0.99	0.9946	0.96	0.9917
318	1.03	0.9928	0.98	0.9945

n_H is Hill's coefficient, r_3 is the linear correlation coefficient of the equation $\lg[Y/(1-Y)] \sim \lg[L]$

3.4 Molecular docking

Molecular docking is an important technique in structural molecular biology and drug discovery with the ability to study the exact binding location of ligands on protein. To further illustrated the interaction mechanism of MEL and PPL, we used molecular simulation technology to further explore this process. The best combination mode predicted by the docking software Autodock 4.2.6 was shown in Fig. 5.

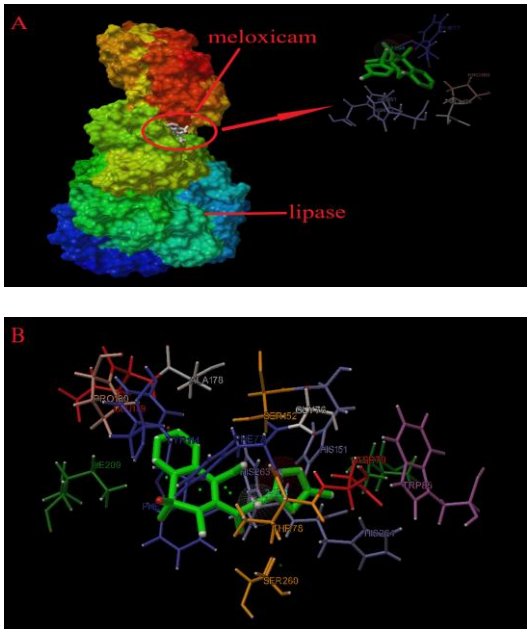

Fig 5: Computation docking model of the interaction between MEL and PPL (A) MEL located within the hydrophobic pocket in PPL (B) Detailed illustration of the amino acid residues lining the binding site in the MEL and PPL cavity

Fig. 5(A) showed the optimal binding configuration of the MEL-PPL system. As could be seen from the docking diagram, the drug molecule MEL was located in the hydrophobic cavity of the PPL. The active center of different lipases usually consists of serine (Ser) residues and histidine (His) residues, and together with aspartic acid (Asp) residues or glutamic acid (Glu) residues constitute a three meta catalytic center [27]. It could be seen from Figure 5(B) that the MEL binding position was near the Asp79, His 263 and Ser152 residues, indicating that the binding of MEL to PPL affected the catalytic activity of PPL. The MEL binding position of the drug molecule was close to the amino acid residues such as Tyr114 and Trp85, which led to the binding of MEL and PPL to effectively quench the endogenous fluorescence of PPL, which was consistent with the synchronous fluorescence experiment.

MEL-PPL system was surrounded by various kinds of hydrophobic residues such as Phe77, Ile209, Ala178, Tyr14, Tyr114 and Trp85, indicating that hydrophobic forces promoted the binding process of MEL to PPL. Furthermore, MEL molecule formed a hydrogen bond with the active residues of Phe77 and the bond length was 2.204 Å. The binding energy obtained from molecular docking for MEL and PPL interaction was -25.76 kJ/mol. Whereas, the free energy change calculated from fluorescence quenching results was -25.08 kJ/mol at 310 K. This difference may be due to exclusion of the solvent in docking simulations or rigidity of the receptor other than Trp and Tyr residues [28]. The energy data obtained by docking the molecules are listed in Table 4. From Table 4, it could be also seen that the electrostatic energy was very much lower than the sum of van der Waals energy, hydrogen bonding energy and desolvation free energy in the binding process of MEL with PPL, indicating that the main interaction mode between MEL and PPL was not electrostatic binding mode. Data from molecular docking could further illustrate that the main types of forces in the MEL-PPL system were hydrophobic interactions and hydrogen bonding.

Table 4: Docking energy of MEL-PPL system (unit: kJ/mol)

Protein PDB ID	ΔG_0[a]	ΔE_1[b]	ΔE_2[c]	ΔE_3[d]
1GPL	-25.76	-29.48	-29.23	-0.25

a: ΔG_0 is the binding energy in the binding process.
b: ΔE_1 denotes intermolecular interaction energy, which is a sum of van der Waals energy, hydrogen bonding energy, desolvation free energy and electrostatic energy.
c: ΔE_2 is the sum of van der Waals energy, hydrogen bonding energy and desolvation free energy.
d: ΔE_3 is the electrostatic energy.

4. Conclusions

In this paper, under the simulated physiological conditions, the interaction mechanism between MEL and PPL was discussed by using synchronous fluorescence spectroscopy and molecular docking technology, and the binding model of MEL-PPL was established. Conventional fluorescence quenching method can only explore the overall properties of the protein-drug system, such as its overall binding constant, the number of binding sites, and the type of force. Synchronous fluorescence spectroscopy can further discuss the Trp residues in drugs and proteins. The interaction between the Trp residue and the Tyr residue give the degree of reaction between the two residues and the drug, and with the help of molecular docking, understand the microenvironmental changes of the amino acid residues around the binding site, in order to provide a new idea to study the mechanism of proteins and drugs.

5. Acknowledgments

The authors gratefully acknowledge the financial support of National Science Foundation of China (Grant no. 21375032).

6. References

1. Franzé JA, Carvalho TF, Gaglieri C, Bannach G, Castro RC, Treu-Filho O, Ionashiro M, Mendes RA. Synthesis, characterization, thermal and spectroscopic studies and bioactivity of complexes of meloxicam with some

bivalent transition metals. Journal of Thermal Analysis & Calorimetry. 2017; 127(2):1393-1405.
2. Sayen S, Carlier A, Tarpin M, Guillon E. A novel copper (II) mononuclear complex with the non-steroidal anti-inflammatory drug diclofenac: structural characterization and biological activity. Journal of Inorganic Biochemistry. 2013; 120(3):39-43.
3. Ebrahimi M, Khayamian T, Hadadzadeh H, Tabatabaei BES, Jannesari Z, Khaksar G. Spectroscopic, biological, and molecular modeling studies on the interactions of [Fe (III)-meloxicam] with G-quadruplex DNA and investigation of its release from bovine serum albumin (BSA) nanoparticles. Journal of Biomolecular Structure and Dynamics. 2015; 33(11):2316-2329.
4. Shantiaee Y, Javaheri S, Movahhedian A, Eslami S, Dianat O. Efficacy of preoperative ibuprofen and meloxicam on the success rate of inferior alveolar nerve block for teeth with irreversible pulpitis. International Dental Journal. 2017; 67(2):85-90.
5. Li CY, Huang ZL, He P, Wu ZQ, Chu ZZ, Wu GH, Zhan FJ. Effect of Isopropanol on Catalytic Kinetics and Molecular Spectrum of Porcine Pancreas Lipase. Chemistry & Bioengineering. 2007; 24(9):46-49.
6. Eom SH. Pancreatic Lipase Inhibitory Activity of Phlorotannins Isolated from Eisenia bicyclis. Phytotherapy Research. 2013; 27(1):148-151.
7. Zhao L, Hu S, Meng Q, Xu M, Zhang H, Liu R. The binding interaction between cadmium-based, aqueous-phase quantum dots with Candida rugosa lipase. Journal of Molecular Recognition Jmr, 2018; 31(46):e2712.
8. Zhang R, Zhao L, Liu R. Deciphering the toxicity of bisphenol a to Candida rugosa lipase through spectrophotometric methods. Journal of Photochemistry & Photobiology B Biology, 2016; 163:40-46.
9. Bagheri H, Madrakian T, Afkhami A. Investigation of the Interaction between Nitrite Ion and Bovine Serum Albumin Using Spectroscopic and Molecular Docking Techniques. Journal of the Chinese Chemical Society, 2014; 61(11):1223-1230.
10. Meti MD, Nandibewoor ST, Joshi SD, More UA, Chaimatadar SA. Binding interaction and conformational changes of human serum albumin with ranitidine studied by spectroscopic and time-resolved fluorescence methods. Journal of the Iranian Chemical Society, 2016; 13(7):1325-1338.
11. Wang XR, Zhu XJ, Liu RM. Study of the interaction between tetramethrin and bovine serum album by synchronous fluorescence spectroscopy. Chemical Research & Application, 2010; 22(6):763-766.
12. Rakotoarivelo NV, Perio P, Najahi E, Nepveu F. Interaction between Antimalarial 2-Aryl-3H -indol-3-one Derivatives and Human Serum Albumin. The Journal of Physical Chemistry B, 2014; 118(47):13477-13485.
13. Gökoğlu E, Yılmaz E. Fluorescence Interaction and Determination of Sulfathiazole with Trypsin. Journal of Fluorescence, 2014; 24(5):1439-1445.
14. Wang Q, Zhang SR, Ji XH. Investigation of interaction of antibacterial drug sulfamethoxazole with human serum albumin by molecular modeling and multi-spectroscopic method. 2014; 124(8):84-90.
15. Yang R, Yu LL, Zeng HJ, Liang RL, Chen XL, Qu LB. The interaction of flavonoid-lysozyme and the relationship between molecular structure of flavonoids and their binding activity to lysozyme. Journal of Fluorescence. 2012; 22(6):1449-1459.
16. Wang CD, Liu BS, Bian G, Zhang HC, Cheng X. Potential influence on drug efficacy from interaction of tartrazine and trypsin. Journal of Photochemistry & Photobiology B Biology. 2018; 51(6):311-317.
17. Karimian MA, Taherikafrani A, Heidarpoor LS, Rastegari AA. Spectroscopic studies of the interaction between alprazolam and apo-human serum transferrin as a drug carrier protein. International Journal of Biological Macromolecules. 2017; 108:263-271.
18. Makarska-Bialokoz M. Interactions of hemin with bovine serum albumin and human hemoglobin: A fluorescence quenching study. Spectrochimica Acta Part A: Molecular and Biomolecular Spectroscopy. 2018; 193(1):23-32.
19. Ma LH, Liu BS, Wang CD, Zhang HC, Cheng X. The interaction mechanism of nifedipine and pepsin. Monatshefte für Chemie-Chemical Monthly. 2018; 149(11):2123-2130.
20. Naik KM, Nandibewoor ST. Spectroscopic studies on the interaction between chalcone and bovine serum albumin. Journal of Luminescence. 2013; 143:484-491.
21. Guo J, Zhong RB, Li WR, Liu YS. Interaction study on bovine serum albumin physically binding to silver nanoparticles: Evolution from discrete conjugates to protein coronas. Applied Surface Science. 2015; 359(5):82-88.
22. Rehman SU, Sarwar T, Ishqi HM, Husain MA, Hasan Z, Tabish M. Deciphering the interactions between chlorambucil and calf thymus DNA: A multi-spectroscopic and molecular docking study. Archives of Biochemistry & Biophysics. 2015; 566(7):7-14.
23. Ross PD, Subramanian S. Thermodynamics of protein association reactions: forces contributing to stability. Biochemistry. 1981; 20(11):3096-3102.
24. Zhou HF, Bi SY, Wang Y, Zhao T. Characterization of the binding of paylean and DNA by fluorescence, UV spectroscopy and molecular docking techniques. Luminescence. 2016; 31(4):1013-1019.
25. Bojko B, SuåKowska A, Maciazek-Jurczyk M, Równicka J, Sułkowski WW. The influence of dietary habits and pathological conditions on the binding of theophylline to serum albumin. Journal of Pharmaceutical & Biomedical Analysis. 2010; 52(3):384-390.
26. Liu BS, Wang J, Xue CL, Yang C, Lv YK. Spectroscopic studies on the interaction of synthetic food colorants with bovine serum albumin. Zeitschrift Fur Physikalische Chemie-International Journal of Research in Physical Chemistry and Chemical Physics, 2011; 225(4):455-468.
27. Fan ZF, Zeng WC, Dai JL, He Q. Interaction of Epigallocatechin-3-gallate with Porcine Pancreas Lipase. Food Science. 2013; 34(7):20-23.
28. Jana S, Dalapati S, Ghosh S. Study of micro heterogeneous environment of protein Human Serum Albumin by an extrinsic fluorescent reporter: a spectroscopic study in combination with Molecular Docking and Molecular Dynamics Simulation. Journal of Photochemistry & Photobiology B Biology. 2012; 112(231):48-58.